

# Incorporating Ephemeral Traffic Waves in A Data-Driven Framework for Microsimulation in CARLA

Alex Richardson  
Computer Science  
Vanderbilt University  
Nashville, TN, USA

william.a.richardson@vanderbilt.edu

Azhar Hasan  
Computer Science  
Vanderbilt University  
Nashville, TN, USA

Gabor Karsai  
Computer Science  
Vanderbilt University  
Nashville, TN, USA

Jonathan Sprinkle  
Computer Science  
Vanderbilt University  
Nashville, TN, USA

jonathan.sprinkle@vanderbilt.edu

**Abstract**—This paper introduces a data-driven traffic microsimulation framework in CARLA that reconstructs real-world wave dynamics using high-fidelity time-space data from the I-24 MOTION testbed. Calibration of road networks in microsimulators to reproduce ephemeral phenomena such as traffic waves for large-scale simulation is a process that is fraught with challenges. This work reconsiders the existence of the traffic state data as boundary conditions on an ego vehicle moving through previously recorded traffic data, rather than reproducing those traffic phenomena in a calibrated microsim. Our approach is to autogenerate a 1 mile highway segment corresponding to I-24, and use the I-24 data to power a cosimulation module that injects traffic information into the simulation. The CARLA and cosimulation simulations are centered around an ego vehicle sampled from the empirical data, with autogeneration of “visible” traffic within the longitudinal range of the ego vehicle. Boundary control beyond these visible ranges is achieved using ghost cells behind (upstream) and ahead (downstream) of the ego vehicle. Unlike prior simulation work that focuses on local car-following behavior or abstract geometries, our framework targets full time-space diagram fidelity as the validation objective. Leveraging CARLA’s rich sensor suite and configurable vehicle dynamics, we simulate wave formation and dissipation in both low-congestion and high-congestion scenarios for qualitative analysis. The resulting emergent behavior closely mirrors that of real traffic, providing a novel cosimulation framework for evaluating traffic control strategies, perception-driven autonomy, and future deployment of wave mitigation solutions. Our work bridges microscopic modeling with physical experimental data, enabling the first perceptually realistic, boundary-driven simulation of empirical traffic wave phenomena in CARLA.

*Index Terms*—

## I. INTRODUCTION

Stop-and-go traffic waves are continuing to be an object of study for advancement in traffic flow theory, and in cyber-physical transportation systems as a means to understand how they can be controlled. While the emergence and propagation of these waves are well-documented in empirical studies and increasingly targeted by control strategies such as adaptive cruise control (ACC), and Vehicle-to-Vehicle (V2V) coordination, there remains a fundamental gap in evaluating the real-world fidelity of mitigation techniques under realistic traffic conditions.

To date, many traffic microsimulations used to study stop-and-go waves rely on abstract road geometries [1], periodic boundary conditions (like ring roads), or synthetic traffic generation. While useful for theoretical exploration or controller training, such environments fall short in replicating the spatiotemporal complexity of real traffic dynamics. Moreover, existing simulation platforms rarely account for the full physical and perceptual realism required to test Autonomous Vehicle (AV) systems under traffic wave conditions.

In this work, we introduce a data-driven, high-fidelity traffic microsimulation in CARLA that reconstructs emergent traffic wave conditions for the ego AV, using empirical data derived from the I-24 MOTION testbed. Our simulation models a 1 mile segment of the I-24 freeway in Tennessee—a corridor that captures vehicle trajectory data at high resolution. The simulation spawns a single ego vehicle from the empirical data at a selected timestamp, longitudinal position, and lane. Surrounding traffic within a longitudinal “visible” range from the ego vehicle is autogenerated and removed via a cosimulation module. The cosimulation module also tracks traffic trajectories in a “ghost cell” region behind and in front of this visible range, which serves as boundary control for the “visible” and ego vehicles. This architecture enables dynamically generated vehicles to enter and exit the area around the ego vehicle in accordance with real-world density profiles extracted from time-space diagrams.

Unlike previous studies that focus on local car-following behavior or theoretical controller performance, our simulation framework targets the fidelity of the full time-space diagram as the primary validation objective. Using CARLA, we simulate traffic dynamics under physically plausible conditions under 2 selected scenarios—a low-congestion and high-congestion scenario—and qualitatively evaluate the simulated ego vehicle’s behavior against the empirical data.

## Contributions

- 1) We develop a CARLA-based traffic microsimulation aligned with a real 1 mile I-24 highway segment, integrating empirical data and road geometry. The software

that executes this coordination between CARLA and the I-24 Motion data is available at [2].

- 2) We demonstrate the first empirically sourced simulation of phantom jam behavior in CARLA, enabling future controller testing, autonomy validation, and policy planning.
- 3) We propose a ghost cell boundary control method for CARLA that enables realistic vehicle injection and exit based on time-space density profiles from real traffic.
- 4) We propose time-space diagram fidelity as a core metric for validating emergent traffic behavior in full 3D AV simulation against real-world data.

## II. RELATED WORK

### A. Stop-and-go Traffic Wave Data and Theory

Extensive research has characterized the behavior of stop-and-go waves empirically in real world highways [3], [4] and in artificial real-world periodic boundary conditions [5]. In part due to the prohibitive cost of obtaining empirical data in the first decades of the field, hydrodynamic and car-following mathematical theories arose to characterize real-world behavior [4], [6], [7]. With the advent of large-scale empirical data [8], statistical tools have also arisen to analyze real-world waves [9].

### B. Control of Stop-and-Go Waves

Many techniques for mitigating stop-and-go waves exist and are in active development. For localized vehicular control, the first major technique emerged in the 1990s in the form of noncooperative Adaptive Cruise Control [10]. While the results of that theory demonstrated approaches that would reduce amplification of disturbances, experimental results showed that manufacturers often were unable to directly implement that theory, resulting in string-unstable commercial systems [11]. Recent research has emerged on various forms of cooperative vehicle stop-and-go wave mitigation, as part of large-scale field experiments [12].

### C. Real World Traffic Flow Data Collection

For decades, microscopic empirical traffic flow data was prohibitive to collect at scale, which hindered development of traffic flow theory and mitigation techniques. Several approaches have converged to ameliorate this in the last decade.

Onboard vehicle data collection by public researchers has indicated that large-scale onboard telemetric data collection can be performed by small-scale research teams, using CAN data collection [13], [14].

Video-based data collection with the advent of computer vision-based tracking has also surged in popularity. Drone-based datasets have become available [15], and recently, I-24 MOTION [16] demonstrated that large-scale microscopic traffic flow data collection is possible from fixed camera poles, with public datasets containing millions of trajectories.

### D. Bird's Eye View Traffic Simulations

Simulations of stop-and-go wave mitigation, for wave analysis, and mitigation technique development, has largely taken the form of Bird's Eye View simulations [17], [18], [19], [20], [21], [1], [22], [23], [24], [25] and macroscopic fluid-dynamic based simulations [26].

However, in recent years, fully immersive 3D Autonomous Vehicle simulators, such as CARLA [27], have become broadly available and feasible to use at scale with hundreds of agents. These offer a diverse selection of potential vehicle and infrastructure models, along with comprehensive meteorological effects. They have been extensively employed in deep RL for end-to-end AV solutions [28], [29], [30], [31]. For traffic stop-and-go wave mitigation, there is great potential for their use, such as in software testing and digital twins.

## III. CARLA COSIMULATION FRAMEWORK

This section details the structure and implementation of the cosimulation architecture built to interface with CARLA for replicating real-world traffic wave dynamics observed on the I-24 freeway. The simulation combines empirical data, realistic road geometry, calibrated vehicle control models, and a novel ghost cell mechanism to recreate emergent stop-and-go phenomena with high physical and behavioral fidelity. CARLA, and the vehicles therein, operate according to CARLA's system design and logic, and are managed by the stock CARLA traffic manager. However, CARLA is partnered with a custom cosimulator module that manages the overall simulation. In this simulation framework, there is an ego vehicle, the visible vehicles - those within a longitudinal distance threshold of the ego vehicle, and the ghost vehicles - the vehicles in the ghost cell regions behind and in front of the ego vehicle.

### A. I-24 Environment

The section of I-24 we use in this simulation study is a 1 mile section, from the 60.6 mile marker, to the 61.6 mile marker. This section of I-24 consists of two straight away roads, one heading southeast away from the Nashville metro area (the "Eastbound" section), and the other heading northwest towards the Nashville metro area (the "Westbound" section). During the morning rush hour, the Westbound section is in high demand, whereas in the afternoon, the Eastbound section experiences the corresponding surge. Both roads have 4 lanes, with the left most lane being a High-Occupancy Vehicle (HOV) lane.

This multi-lane highway section has minimal curvature, and no interchanges or ramps, ensuring that emergent traffic phenomena are primarily impacted by vehicle behavior and vehicle inflow/outflow constraints.

### B. Road and Environment Generation

To generate the roads and terrain, we use a custom in-house map generator to procedurally create a basic terrain mesh, along with the 1 mile I-24 highway section. This generates an elevation-aware road topography, along with all the relevant lanes.

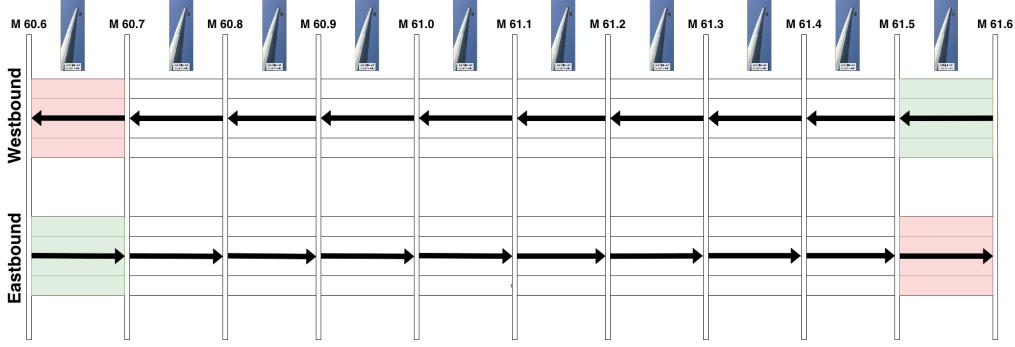


Fig. 1: The I-24 60.6 mile to 61.6 mile region shown as a simplified diagram, with each segment at 0.1 mile in length demarcated. Cameras are shown at approximate spacing, with the green segments showing the beginning of each road, and the red segments showing the end of each road.

Road surface friction directly uses the stock CARLA road surface friction parameters. Lane markings and signs are not generated for the purposes of this simulation study.

Meteorological conditions consist of CARLA's default "high noon" setting, with no precipitation.

### C. Cosimulator Design

1) *Vehicle State*: Each vehicle instantaneous state with the identifier  $id$  is designated as  $\overset{id}{v}$ . Each vehicle has the corresponding internal state:

- $\overset{id}{v}_t$ : The vehicle's current unix timestamp in seconds.
- $\overset{id}{v}_x$ : The vehicle's current longitudinal position on the road in meters as described in Figure 1.
- $\overset{id}{v}_y$ : The vehicle's current lateral position on the road in meters as described in Figure 1.
- $\overset{id}{v}_l$ : The vehicle's current lane - in this work,  $l \in \{-1, -2, -3, -4\}$ :  $-1$  corresponds to the leftmost lane (which is HOV), and  $-4$  corresponds to the rightmost lane. The identifiers descend in a left to right order.
- $\overset{id}{v}_{vel}$ : The vehicle's current longitudinal velocity in  $\frac{m}{s}$ .

2) *Configuration*: There are several configuration options the cosimulator has:

- Episode time-length ( $t_{max}$ ): The total time length of the simulation, in seconds. By default, it is 30 seconds.
- Time-step size ( $\Delta t$ ): This is the size, in seconds, of the time-steps of both the CARLA simulation and the cosimulation module. By default, it is 0.01 seconds.
- Default desired speed ( $vel_{default}$ ): The default desired speed in  $\frac{m}{s}$  for the ego and visible vehicles in CARLA.
- Desired initial road ( $r$ ): This is the selected roadway we want our vehicle to be simulated on. In this work,  $r \in \{\text{Westbound}, \text{Eastbound}\}$  - it is either the Westbound road, or the Eastbound road.
- Visible window ( $w_{visible}$ ): This is the longitudinal window, in meters, for the visible vehicles. By default, it is 150 meters. This extends from the ego vehicle's longitudinal location ( $\overset{ego}{v}_x$ ) both backwards and forwards

with respect to the direction of travel. This means the bounds of the  $v_x$  of any visible vehicle are:

$$\overset{ego}{v}_x - w_{visible} \leq v_x \leq \overset{ego}{v}_x + w_{visible}$$

- Ghost window ( $w_{ghost}$ ): This is the longitudinal window, in meters, for the ghost vehicles. By default, this is 50 meters. These are placed immediately in front and behind of the visible window.

Hence, the bounds of the  $v_x$  of any ghost vehicle are:

$$\overset{ego}{v}_x - w_{visible} - w_{ghost} \leq v_x \leq \overset{ego}{v}_x - w_{visible}$$

or:

$$\overset{ego}{v}_x + w_{visible} \leq v_x \leq \overset{ego}{v}_x + w_{visible} + w_{ghost}$$

- Desired initial lane, x, and timestamp ( $\overset{ego}{v}_l$ ,  $\overset{ego}{v}_x$ ,  $\overset{ego}{v}_t$ ): This is the lane, longitudinal position, and timestamp we desire for our selected ego vehicle in the initialization phase.

3) *Simulation State*: The simulation's internal state consists of the following:

- Current timestamp ( $t$ ): The current unix timestamp, in seconds, of the simulation.
- Timestamp origin ( $t_0$ ): This is the first unix timestamp of the simulation. Corresponds directly to the original timestamp of the selected ego vehicle from the empirical data.
- Ego vehicle ( $\overset{ego}{v}$ ): The ego vehicle of the simulation.
- Visible vehicle set ( $V_{visible}$ ): The current set of  $\overset{id}{v}$  that are currently in the visible range, spawned in CARLA, and behaviorally largely managed by the Traffic Manager (except for desired velocity).
- Ghost vehicle set ( $V_{ghost}$ ): The current set of  $\overset{id}{v}$  that are currently in the ghost cells, and updated by reloading them from the I-24 empirical data at each loop (see below).
- I-24 Empirical Dataset ( $V_{empirical}$ ): This is the total set of timestamped instantaneous vehicle state data, corresponding in format to  $\overset{id}{v}$ , that is available. We use this to

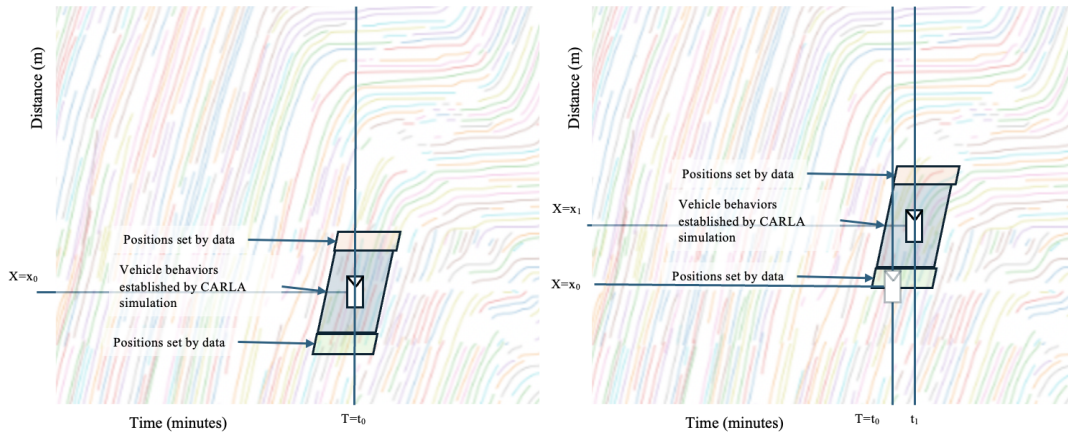


Fig. 2: Two time-space diagrams with overlay of the ego vehicle and its surroundings at two time,  $t_0$  and  $t_1$ . The direction of travel is “up” in the figure, and time advances to the right. (Left) at time  $T = t_0$ . Downstream cars are placed in their exact positions and given their velocity directly based on the representative traffic data. The simulated cars in CARLA are in the immediate surroundings of the ego vehicle, and managed by its traffic control framework. Upstream cars (lower in the figure) are positioned directly by data. (Right) at time  $T = t_1$  the ego car and its surroundings have moved downstream. The car has now encountered a traffic wave, which means that additional cars will begin to appear in the local CARLA framework as the surroundings pick those cars up directly from the positional information gained by the measured data.

spawn the ego/visible/ghost vehicles in the first timestep, and update the ghost region as the simulation advances.

4) *CARLA Vehicles*: The ego vehicle and the visible vehicles are the only vehicles that are ever spawned and operated within CARLA itself - ghost vehicles are never created. The vehicle type for each vehicle in CARLA is randomly selected. All are controlled by CARLA’s Traffic Manager. When spawned, each is given an instantaneous velocity by an appropriate impulse force.

5) *Simulation Control Flow*: The simulation performs the following steps:

- 1) Initialize  $\tilde{v}^{ego}$  to the spatiotemporally closest vehicle available in  $V_{empirical}$ . Set the timestamp origin  $t_0$  and current timestamp  $t$  to  $\tilde{v}^{ego}_t$ .
- 2) Load into  $V_{visible}$  and ghost vehicles  $V_{ghost}$  all eligible vehicles from  $V_{empirical}$  at timestamp  $t$  that are not  $\tilde{v}^{ego}$ . Spawn the ego/visible vehicles into CARLA as appropriate.
- 3) Update the CARLA Traffic Manager’s desired velocity for each ego and visible vehicle. Ego vehicle is maintained at the default speed  $vel_{default}$ . Visible vehicles behind the ego vehicle are given the same speed. For visible vehicles ahead of the ego vehicle, it is more complex. If they are not the lead vehicle for their lane, their desired speed is the default speed. If they are the lead vehicle for their lane of visible vehicles, their desired velocity corresponds to the ahead ghost vehicle. If that ghost vehicle doesn’t exist, it is the default speed.
- 4) Step the CARLA simulation by  $\Delta t$ . All of  $\tilde{v}^{ego}$ ,  $V_{visible}$  are updated appropriately. All  $V_{ghost}$  vehicles have their longitudinal positions temporally advanced by their velocity to account for their movement as well.

- 5) If a  $\tilde{v}^{id} \in V_{visible}$  is now in the ghost regions, assign it internally to  $V_{ghost}$  and despawn it in CARLA.
- 6) If a  $\tilde{v}^{id} \in V_{ghost}$  is now in the visible region, assign it internally to  $V_{visible}$  and spawn it in CARLA.
- 7) Completely reload the  $V_{ghost}$  from  $V_{empirical}$  according to the current longitudinal ghost bounds and timestamp.
- 8) If  $t \geq (t_0 + t_{max})$ , terminate the simulation. Otherwise, return to step 4.

## IV. EVALUATION AND RESULTS

### A. I-24 Empirical Dataset

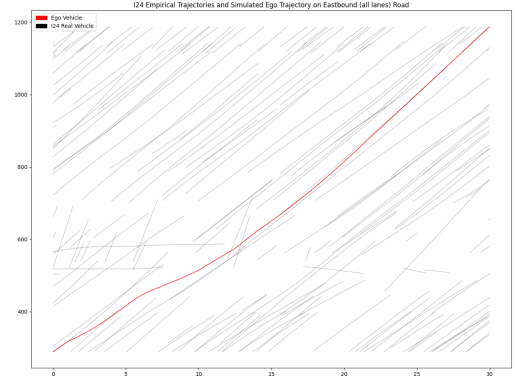
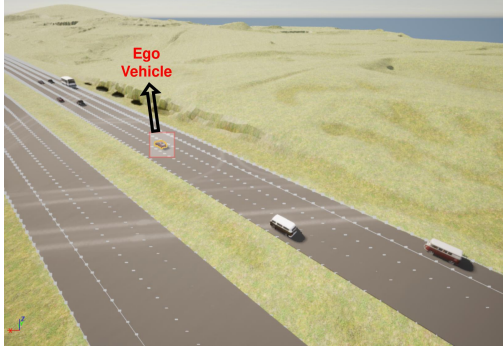
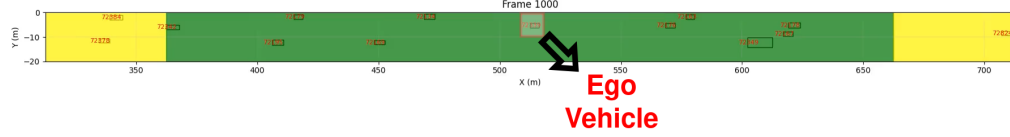
Our empirical dataset we use for evaluation is sourced directly from the 2022 I-24 MOTION dataset between the 60.6 and 61.6 mile markers. We select 7 days - 22nd, 23rd, 24th, 25th, 28th, 29th, and 30th of November 2022. Each day lasts between 6 AM and 10 AM CST - which results in 28 hours of potential re-playability.

### B. Qualitative Experiments

1) *Scenario A*: Scenario A is a 30 second simulation, with the selected ego vehicle on the eastbound road, 2nd lane to the left, at position  $x = 300$  meters longitudinally along our 1 mile road, at 6:45:50 AM on November 30th, 2022. The eastbound road is in low-congestion, serving as an excellent baseline. The results of the simulation are shown in Figure 3. The results are consistent with the empirical trajectories.

2) *Scenario B*: Scenario B is a 30 second simulation, with the selected ego vehicle on westbound road, the 1st (HOV) lane to the left, at position  $x = 700$  meters longitudinally along our 1 mile road, at 6:45:50 AM on November 30th, 2022. In the empirical data, there is a prominent stop-and-go wave beginning to move through the ego vehicle’s position on the

(a) Bird's eye view of the cosimulation state at  $t=10$ . Green indicates the visible vehicle region, and yellow indicates the ghost cells.

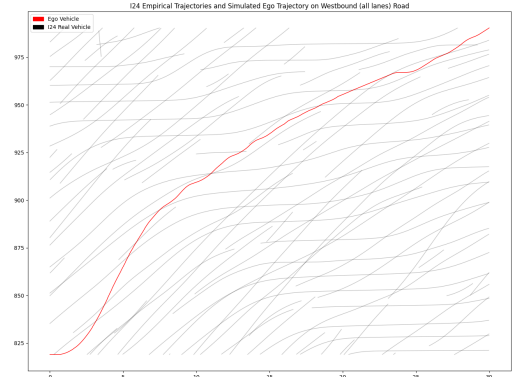
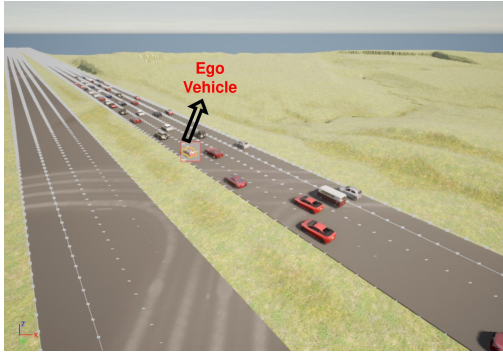
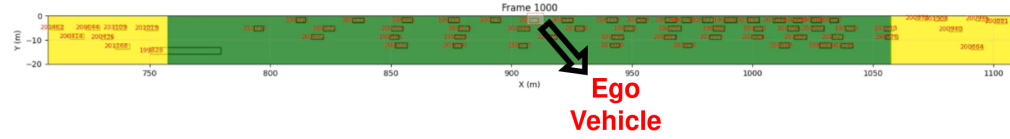


(b) Screenshot of the CARLA simulation at  $t=10$ . Ego vehicle highlighted.

(c) Time-space diagram of the I-24 Empirical Trajectories (all lanes) vs the Simulated Ego Trajectory.

Fig. 3: Scenario A simulation results - a Bird's Eye View of the cosimulation state at (a), a screenshot of CARLA at (b) and a time-space diagram showing the simulated ego vehicle's trajectory vs the I24 empirical trajectories at (c).

(a) Bird's eye view of the cosimulation state at  $t=10$ . Green indicates the visible vehicle region, and yellow indicates the ghost cells.



(b) Screenshot of the CARLA simulation at  $t=10$ . Ego vehicle highlighted.

(c) Time-space diagram of the I-24 Empirical Trajectories (all lanes) vs the Simulated Ego Trajectory.

Fig. 4: Scenario B simulation results - a Bird's Eye View of the cosimulation state at (a), a screenshot of CARLA at (b) and a time-space diagram showing the simulated ego vehicle's trajectory vs the I24 empirical trajectories at (c).

HOV lane, with minimal disruption to the 3rd and 4th lanes. Thus, this is an excellent showcase of how the simulation processes stop-and-go waves. The results are shown in Figure 4. The simulated ego vehicle's behavior deviates from the empirical data - it does not come to a near-stop. Instead, it merely slows, which is the behavior of the two rightmost lanes

in the empirical data. This is due to CARLA's traffic manager inducing vehicles on the HOV lane to lane change into the less congested lanes, improving flow compared to the empirical data. Furthermore, the ego velocity starts at  $0 \frac{m}{s}$ . This is due to inconsistencies of the efficacy of the impulse-based method for instantaneous acceleration as discussed before.



### C. Discussion

These results indicate the ability of this simulation framework to closely mirror the empirical traffic data ingested from I-24 MOTION, but also illustrate the limitations of the stock behavioral models employed for the “visible” vehicles. Since they use CARLA’s Traffic Manager, they are not employing IDM. Rather, the behaviors are based on heuristic models from CARLA, which may not reflect the family of behaviors in human drivers. Special lanes in this simulation schema, such as HOV lanes, are treated equally to other lanes, which exacerbates the sim-to-real gap. Thus, in order to improve the behavioral realism of this simulation framework, custom IDM-based agents and lane-changing logic will need to be deployed within it for future work.

### V. CONCLUSION AND FUTURE WORK

In this work, we presented a data-driven traffic microsimulation framework in CARLA that uniquely reconstructs real-world wave dynamics for a local ego vehicle. “Visible” traffic in the ego vehicle’s vicinity is able to be directly modeled in CARLA, but still updated and constrained by the global empirical traffic data by the cosimulation module. This will empower future controller testing, autonomy validation, and more. Furthermore, large-scale mesoscopic empirical data allows the fidelity of such microsimulations to be directly evaluated against that data.

Future work will focus on closing the sim-to-real gap in CARLA’s Traffic behavioral models. Our goal is to directly employ such simulations for RL-training of wave-dissipation models, and more. Additional effort will be devoted to analysis of the mathematical framework for convolution of the existing traffic data as ghost cell inputs, to reduce variability of vehicles entering and leaving those cells, which may cause discretized responses in following vehicles. Future work may be able to smooth these disruptions in order to more closely replicate the experience on the open road.

### REFERENCES

- [1] C. Wu, A. R. Kreidieh, K. Parvate, E. Vinitzky, and A. M. Bayen, “Flow: A modular learning framework for mixed autonomy traffic,” *IEEE Transactions on robotics*, 2021.
- [2] Anonymous, “I-24 motion to carla helpers.” [Online]. Available: [https://github.com/AlexOSAdventurer/i24motion\\_to\\_carla\\_helpers](https://github.com/AlexOSAdventurer/i24motion_to_carla_helpers)
- [3] M. Treiber and A. Kesting, “Traffic flow dynamics,” 2012.
- [4] M. Treiber, A. Hennecke, and D. Helbing, “Congested traffic states in empirical observations and microscopic simulations,” *Physical Review E*, 2000.
- [5] Y. Sugiyama, M. Fukui, M. Kikuchi, K. Hasebe, A. Nakayama, K. Nishinari, S.-i. Tadaki, and S. Yukawa, “Traffic jams without bottlenecks—experimental evidence for the physical mechanism of the formation of a jam,” 2008.
- [6] P. G. Gipps, “A behavioural car-following model for computer simulation,” *Transportation Research Part B-methodological*, 1981.
- [7] M. Bando, K. Hasebe, A. Nakayama, A. Shibata, and Y. Sugiyama, “Dynamical model of traffic congestion and numerical simulation,” *Physical review. E, Statistical physics, plasmas, fluids, and related interdisciplinary topics*, 1995.
- [8] D. Gloudemans, Y. Wang, J. Ji, G. ZachÄr, W. Barbour, E. Hall, M. Cebelak, L. Smith, and D. B. Work, “I-24 motion: An instrument for freeway traffic science,” *Transportation Research Part C: Emerging Technologies*, vol. 155, p. 104311, 2023. [Online]. Available: <https://www.sciencedirect.com/science/article/pii/S0968090X23003005>
- [9] J. Ji, D. Gloudemans, Y. Wang, G. ZachÄr, W. Barbour, J. Sprinkle, B. Piccoli, and D. B. Work, “Scalable analysis of stop-and-go waves,” *arXiv.org*, 2024.
- [10] P. Ioannou and C. Chien, “Autonomous intelligent cruise control,” 1993.
- [11] G. Gunter, D. Gloudemans, R. Stern, S. T. McQuade, R. Bhadani, M. Bunting, M. L. D. Monache, R. Lysecky, B. Seibold, J. Sprinkle, B. Piccoli, and D. B. Work, “Are commercially implemented adaptive cruise control systems string stable?” *arXiv (Cornell University)*, 2019.
- [12] J. W. Lee *et al.*, “Traffic control via connected and automated vehicles (cavs): An open-road field experiment with 100 cavs,” *IEEE Control Systems*, 2025.
- [13] M. Bunting, R. Bhadani, and J. Sprinkle, “Libpanda: A high performance library for vehicle data collection,” *Proceedings of the Workshop on Data-Driven and Intelligent Cyber-Physical Systems*, 2021.
- [14] S. Elmadani, M. Nice, M. Bunting, J. Sprinkle, and R. Bhadani, “From can to ros: A monitoring and data recording bridge,” *Proceedings of the Workshop on Data-Driven and Intelligent Cyber-Physical Systems*, 2021.
- [15] R. Krajewski, J. Bock, L. Kloecker, and L. Eckstein, “The highd dataset: A drone dataset of naturalistic vehicle trajectories on german highways for validation of highly automated driving systems,” *International Conference on Intelligent Transportation Systems*, 2018.
- [16] D. Gloudemans, Y. Wang, J. Ji, G. ZachÄr, W. Barbour, and D. B. Work, “I-24 motion: An instrument for freeway traffic science,” *arXiv (Cornell University)*, 2023.
- [17] M. Treiber and A. Kesting, “The intelligent driver model with stochasticity—new insights into traffic flow oscillations,” *Transportation Research Part B: Methodological*, 2017.
- [18] X. Di and R. Shi, “A survey on autonomous vehicle control in the era of mixed-autonomy: From physics-based to ai-guided driving policy learning,” *Transportation Research Part C: Emerging Technologies*, 2021.
- [19] P. A. Lopez, E. Wiebner, M. Behrisch, L. Bieker-Walz, J. Erdmann, Y.-P. FlötterÄd, R. Hilbrich, L. LÄ¼cken, J. Rummel, and P. Wagner, “Microscopic traffic simulation using sumo,” *International Conference on Intelligent Transportation Systems*, 2018.
- [20] E. Vinitzky, A. Kreidieh, L. L. Flem, N. Kheterpal, K. Jang, C. Wu, F. Wu, R. Liaw, and E. Liang, “Benchmarks for reinforcement learning in mixed-autonomy traffic,” *Conference on Robot Learning*, 2018.
- [21] C. Wu, A. Kreidieh, K. Parvate, E. Vinitzky, and A. M. Bayen, “Flow: Architecture and benchmarking for reinforcement learning in traffic control,” *arXiv.org*, 2017.
- [22] J. Laval, C. Toth, and Y. Zhou, “A parsimonious model for the formation of oscillations in car-following models,” *Transportation Research Part B-methodological*, 2014.
- [23] M. Zhou, X. Qu, and X. Li, “A recurrent neural network based microscopic car following model to predict traffic oscillation,” *Transportation Research Part C-emerging Technologies*, 2017.
- [24] S. Panwai and H. Dia, “Neural agent car-following models,” *IEEE Transactions on Intelligent Transportation Systems*, 2007.
- [25] M. Sharath and N. R. Velaga, “Enhanced intelligent driver model for two-dimensional motion planning in mixed traffic,” *Transportation Research Part C-emerging Technologies*, 2020.
- [26] D. Zehe, D. Grotzky, H. Aydt, W. Cai, and A. Knoll, “Traffic simulation performance optimization through multi-resolution modeling of road segments,” *SIGSIM-PADS*, 2015.
- [27] A. Dosovitskiy, G. Ros, F. Codevilla, A. M. Lopez, and V. Koltun, “Carla: An open urban driving simulator,” *arXiv: Learning*, 2017.
- [28] Q. Chao, H. Bi, W. Li, T. Mao, Z. Wang, M. C. Lin, and Z. Deng, “A survey on visual traffic simulation: Models, evaluations, and applications in autonomous driving,” *Computer graphics forum (Print)*, 2020.
- [29] R. P. Bhattacharyya, D. J. Phillips, B. Wulfe, J. Morton, A. Kuefler, and M. J. Kochenderfer, “Multi-agent imitation learning for driving simulation,” *IEEE/RJS International Conference on Intelligent Robots and Systems*, 2018.
- [30] B. Osinski, P. Milos, A. Jakubowski, P. Ziecina, M. Martyniak, C. Galias, A. Breuer, S. Homoceanu, and H. Michalewski, “Carla real traffic scenarios - novel training ground and benchmark for autonomous driving,” *arXiv.org*, 2020.
- [31] Z. Xu, X. Wang, X. Wang, and N. Zheng, “Safety validation for connected autonomous vehicles using large-scale testing tracks in high-fidelity simulation environment,” *Accident Analysis & Prevention*, 2025.